# Effect of the subsurface oxygen diffusion on the Ziff-Gulari-Barshad catalytic reaction model

B. C. S. Grandi and W. Figueiredo*
*Departamento de Física, Universidade Federal de Santa Catarina, 88040-900 Florianópolis, Santa Catarina, Brazil*
(Received 1 October 2001; revised manuscript received 20 November 2001; published 5 March 2002)

We study a version of the Ziff-Gulari-Barshad model where we include the diffusion of oxygen atoms between the uppermost layer and the subsurface. When a CO molecule impinges the surface, it occupies a single site, while the $O_2$ molecule needs two neighboring sites to be adsorbed. The oxidation of the CO molecule occurs only at the top layer, and this happens whenever a CO molecule is nearest neighbor of an O atom. Through the pair mean-field approximation we determine the phase diagram of the model for different values of the diffusion rate of oxygen atoms between the subsurface and the top layer. The diagram exhibits a continuous line that separates regions displaying O-poisoned and non-O-poisoned states. We show that above a critical value of the diffusion rate of oxygen atoms from the subsurface to the top layer, there is no more oxygen poisoning for any nonzero value of the diffusion rate from the top layer to the subsurface. This behavior is also verified in Monte Carlo simulations.

DOI: 10.1103/PhysRevE.65.036135 PACS number(s): 05.70.−a, 82.65.+r

## I. INTRODUCTION

The well-known model introduced by Ziff-Gulari-Barshad (ZGB model) [1] to explain the catalytic oxidation of CO shows some features that are not in agreement with the experiments. One such case is related to the appearance of a continuous phase transition between an active and an O-poisoned states. Experiments indicate that a reactive state appears as soon as CO molecules start to impinge the catalytic surface [2]. Some attempts were made with the aim to clarify this point [2–9]. For instance, Khan *et al.* [7] proposed a model where the oxygen atoms may be also adsorbed into the subsurface. In their model, besides the usual mechanism of Langmuir-Hinshelwood applied to the surface, they included three new steps involving the oxygen atoms:

(a) An oxygen molecule can be adsorbed with one atom sitting on the top layer and the other one in the layer immediately under the top layer.

(b) A CO molecule adsorbed in the top layer can also react with an oxygen atom of the subsurface.

(c) Oxygen atoms can diffuse between the topmost layer and the subsurface.

In their model the continuous transition between the active and O-poisoned states disappears in two possible situations: (i) if we do not consider the diffusion mechanism, the CO oxidation necessarily involves an oxygen atom of the subsurface and the $O_2$ molecules are adsorbed occupying sites on the top layer and at the subsurface; (ii) if the diffusion mechanism is considered, for suitable values of diffusion rates. As pointed out by these authors, although the disappearance of the continuous transition is closer to the experimental findings, the production of $CO_2$ involving a subsurface oxygen atom has not been reported experimentally. Recently, D'Ajello *et al.* [10] studied the transient oxidation of CO over a catalyst in the presence of subsurface oxygen atoms: in this case the subsurface was modeled by 20 monolayers and the oxidation of CO occurs only with oxygen atoms at the topmost layer.

In this paper we consider a variation of the ZGB model by introducing the diffusion of oxygen atoms between the top layer and the subsurface. The deposition of the CO and $O_2$ molecules proceeds in the same way as seen in the ZGB model: both molecules are adsorbed only at the uppermost layer and the oxidation of CO occurs involving only oxygen atoms at the top layer. We believe our model is more realistic than then one proposed by Khan *et al.* [7] because we do not need to include the oxygen atoms of the subsurface to explain the formation of $CO_2$. The model is studied within site and pair mean-field approximations, and we determine the coverages of the species at the surface and subsurface as a function of the deposition rate of CO molecules and of the diffusion rates of O between the layers. We show that, in the pair mean-field approximation, the continuous phase transition into the absorbing state disappears for suitable values of the diffusion rates. We also observed that the first-order transition into CO-poisoned state is insensitive to the diffusion rates between the layers. In the following section, we present the model, the reaction and diffusion steps, and the equations of motion in the pair mean-field approximation. In Sec. III we present the results obtained for the coverages and the phase diagram within the pair approximation calculations along with some Monte Carlo simulations. Our conclusions are presented in Sec. IV.

## II. MODEL AND PAIR APPROXIMATION

In the ZGB surface reaction model, molecules of CO and $O_2$ are adsorbed on a catalyst, represented by a square lattice, according to their partial pressures in the gaseous phase. The whole process follows the Langmuir-Hinshelwood mechanism and the following three steps must be considered:

$$(1)\quad \mathrm{CO}(g)+V\rightarrow \mathrm{CO}(a),$$

$$(2)\quad \mathrm{O_2}(g)+2V\rightarrow 2\mathrm{O}(a),$$

$$(3)\quad \mathrm{CO}(a)+\mathrm{O}(a)\rightarrow \mathrm{CO_2}(g)+2V,$$

*Email address: wagner@fisica.ufsc.br

 

TABLE I. All the possible transitions among pairs of species (O, CO, and $V$).

| From: | $VV$ | $VC$ | $VO$ | $VO_S$ | $VV_S$ | $CC$ | $CV_S$ | OO | $OO_S$ | $OV_S$ | $V_SO_S$ | $V_SV_S$ | $O_SC$ | $O_SO_S$ |
|---|---|---|---|---|---|---|---|---|---|---|---|---|---|---|
| To: $VV$ | | $R_1$ | $R_2$ | | | $R_3$ | | | | | | | | |
| $VC$ | $R_4$ | | | | | $R_5$ | | | | | | | | |
| $VO$ | $R_6$ | | | | | | | $R_7$ | | | | | | |
| $VO_S$ | | | | | | | | | $R_8$ | $R_9$ | | | $R_{10}$ | |
| $VV_S$ | | | | | | | $R_{11}$ | | | $R_{12}$ | | | | |
| $CC$ | | $R_{13}$ | | | | | | | | | | | | |
| $CV_S$ | | | | | $R_{14}$ | | | | | | | | | |
| OO | $R_{15}$ | | $R_{16}$ | | | | | | | | | | | |
| $OO_S$ | | | | $R_{17}$ | | | | | | | | | | |
| $OV_S$ | | | | $R_{18}$ | $R_{19}$ | | | | | | | | | |
| $V_SO_S$ | | | | | | | | | | | | $R_{20}$ | | $R_{21}$ |
| $V_SV_S$ | | | | | | | | | | | $R_{22}$ | | | |
| $O_SC$ | | | | $R_{23}$ | | | | | | | | | | |
| $O_SO_S$ | | | | | | | | | | | $R_{24}$ | | | |

where the labels $a$ and $g$ denote adsorbed and gaseous particles, respectively, and $V$ is a vacant site. The steps (1) and (2) describe the adsorption of the molecules CO and $O_2$, respectively, and the third step represents the proper reaction between the adsorbed species to form the $CO_2$ molecule. When the $O_2$ molecule arrives at the surface, it dissociates completely. The formation of $CO_2$ molecule occurs only if CO and O are nearest neighbors on the lattice. $CO_2$ molecules are assumed to leave the lattice immediately, so that the production of $CO_2$ leaves two new empty sites for possible new adsorption. When we take into account the diffusion of oxygen atoms between the surface and the subsurface, we include one more step:

$$(4) \quad O(a)+V_S \rightleftharpoons O_S+V,$$

where $O_S$ and $V_S$ mean an oxygen and a vacant site in the subsurface, respectively.

To describe the whole process we need to consider the relative adsorption rate of CO molecules, denoted by $y_{CO}$, and the diffusion rates of oxygen: $d_1$ is the diffusion rate from the top layer to subsurface, and $d_2$ is the diffusion rate from the subsurface to the surface.

Let us now turn to describe the equations of motion in the pair mean-field approximation. In this work we do not show the results based on the site approximation because they do not introduce any novelty. For instance, as it is well known [11], the site approximation applied to the ZGB model gives non-O-poisoned states for any value of $y_{CO}$, contrary to the results of the Monte Carlo simulations and the pair approximation. The inclusion of the diffusion of O between the layers does not change this picture. On the other hand, we will show that the inclusion of the diffusion rates $d_1$ and $d_2$, in the pair approximation, changes the critical point of the transition between the active and the O-poisoned state. In this approximation we introduce the correlation between two nearest neighbor sites of the lattice. This correlation is defined by the conditional probability $P(i|j)$, which is the probability that a given site to be of type $i$, given that one of its nearest neighbors is of type $j$. In this way, the probability of a given pair $p_{ij}$ is given by $p_{ij}=p_jP(i|j)$, where $p_j$ is the density of sites occupied by a species $j$ ($j$ means an oxygen, a CO molecule or a vacant site).

The equations of motion are obtained by writing the gain-loss rate equations for the pair probabilities, which are evaluated by counting the changes in the number of nearest neighbor pairs in a neighborhood of sites centered on, and including, the center pair $ij$. For this model that includes the subsurface, we need to consider 14 independent pair probabilities: $p_{VV}$, $p_{VC}$, $p_{VO}$, $p_{CC}$, $p_{OO}$, $p_{VO_S}$, $p_{VV_S}$, $p_{O_SC}$, $p_{CV_S}$, $p_{OO_S}$, $p_{OV_S}$, $p_{V_SO_S}$, $p_{V_SV_S}$, $p_{O_SO_S}$. The label $S$ indicates a site in the subsurface, and C means a CO molecule. The pairs $(ij)$ and $(ji)$, although physically distinct, contribute with the same weight to the equations of motion. All these pair probabilities are related to the density of the species O and CO and to the density of vacant sites by equations of the type $p_j=\Sigma_i p_{ij}$. Table I shows all the possible transitions among the pairs. For instance, $R_1$ is the transition rate for the central pair $VC$ to change to a new configuration $VV$. This process can occur by two independent paths: (a) the $O_2$ molecule is adsorbed on the top layer, and one of its oxygen atoms occupies a vacant site, which is nearest neighbor of the CO molecule of the central pair; (b) an oxygen atom at the subsurface migrates to a nearest neighbor vacant site of the CO molecule at the top layer. In the Appendix we present the explicit expressions for the transition rates.

The equation of motion for the $p_{VC}$ pair density is

$$\frac{dp_{VC}}{dt}=R_4+R_5-(R_1+R_{13}), \tag{1}$$

which can be read from row 2 and column 2 of Table I. Similar expressions can be written for the other 13 pair densities. The set of 14 equations for the pair probabilities cannot be solved analytically. We integrate this system of equations by the fourth-order Runge-Kutta method, with the

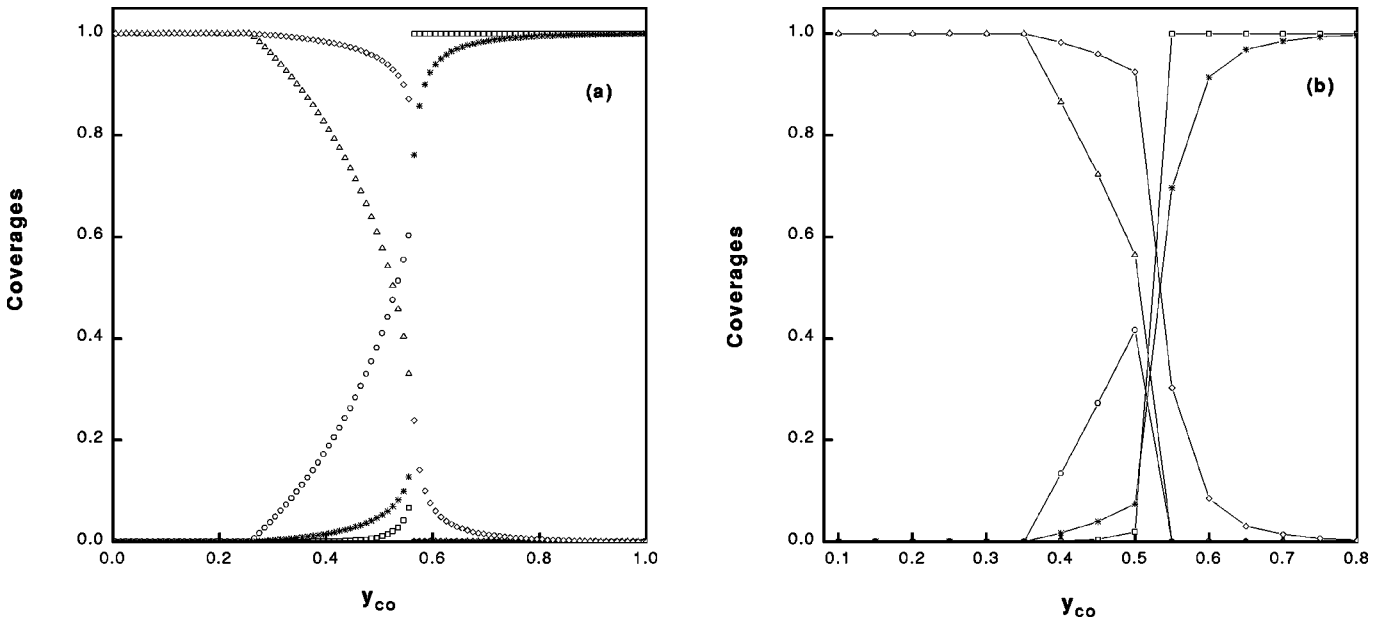


FIG. 1. Coverages at the surface and subsurface as a function of $y_{CO}$. Square (CO), circle ($V$ at surface), triangle (O at surface), diamond (O at subsurface), and star ($V$ at subsurface). The downward diffusion coefficent is $d_1=0.1$ and the upward diffusion coefficient is $d_2=0.01$. (a) Pair approximation; (b) Monte Carlo simulations (the curves serve as guides to the eye).

initial condition of an empty lattice. In our calculations, we take $p_V<10^{-6}$ as being a nonactive state.

### III. COVERAGES AND PHASE DIAGRAM

Figure 1(a) exhibits the pair approximation coverages at the surface and subsurface as a function of $y_{CO}$ for $d_1=0.1$ (downward diffusion of the oxygen atoms) and $d_2=0.01$ (upward diffusion of the oxygen atoms). For these values of the diffusion parameters, the continuous phase transition between the active and the O-poisoned state occurs at the value $y_1=0.245$. This value is almost the same obtained in the absence of diffusion by Dickman [11] in the pair approximation, $y_1=0.2497$. Although the pair approximation gives only mean-field-like critical properties, it is a good formulation to obtain a qualitative picture of the phase transitions. A successful application of the pair approximation can also be seen in the work of Zhonghuai *et al.* [12] where a dimer-dimer surface reaction model was studied. The simulations performed by Ziff, Gulari, and Barshad gave the value $y_1=0.389$. On the other hand, concerning the first-order transition, we also observe that the transition point $y_2$ is insensitive to the diffusion parameters: in the absence of the diffusion, simulations give $y_2=0.525$ and pair approximation $y_2=0.561$; for the diffusion parameters of Fig. 1(a) we found $y_2=0.555$. As expected, the coverage of O at the subsurface exhibits the same behavior as the coverage of this species at the surface. That is, a continuous transition is observed at the same point $y_1=0.245$. However, after we cross the transition point $y_1$, the content of oxygen atoms at the subsurface decreases continuously, even when we cross the first-order transition point $y_2$. For values of $y_{CO}$ larger than $y_2$, while the surface is poisoned by CO, the subsurface still presents some sites occupied by oxygen atoms. This result is due to the fact that we have integrated our equations with the initial condition of an empty lattice.

We have also performed Monte Carlo simulations for this model. We used two layers of square lattices with linear dimension $L=40$ in each layer. We started all simulations with both layers empty and used periodic boundary conditions. For each value of the deposition rate $y_{CO}$ of the CO molecules, we generate a random number to know what molecule will be deposited in the next step. If we choose CO, a site at the top layer is chosen at random for deposition; if it is empty the deposition occurs, otherwise not. For the deposition of $O_2$, also at the top layer, we need to choose at random a pair of nearest neighbors; deposition occurs only if this pair is found, and after deposition the $O_2$ molecules dissociate so that the two O atoms are free to react independently. In both situations, after any event of deposition, we need to search for nearest neighbor pairs of CO and O. If a pair similar to this is found, they react forming a $CO_2$ molecule that leaves the surface, freeing two new sites at the top layer. The diffusive movement of oxygen atoms between the layers is also considered. The diffusion is only permitted between pairs of sites that are nearest neighbors in both layers. For a diffusion of an O atom to the subsurface, with a diffusion rate $d_1$, a random O is chosen at the top layer, and the diffusion is successful only if there is an empty site just below the O atom. For an upward diffusion of O, with a diffusion rate $d_2$, we first select at random an O atom in the subsurface. If the site on the top layer just over this O atom is occupied, the diffusion is not permitted. On the other hand, if the site is vacant, the diffusion occurs and we immediately search for its CO nearest neighbors to react.

As usual in Monte Carlo simulations, the time is measured in appropriate MCu (Monte Carlo units). For a given experiment, we defined the Monte Carlo unit by the sum of

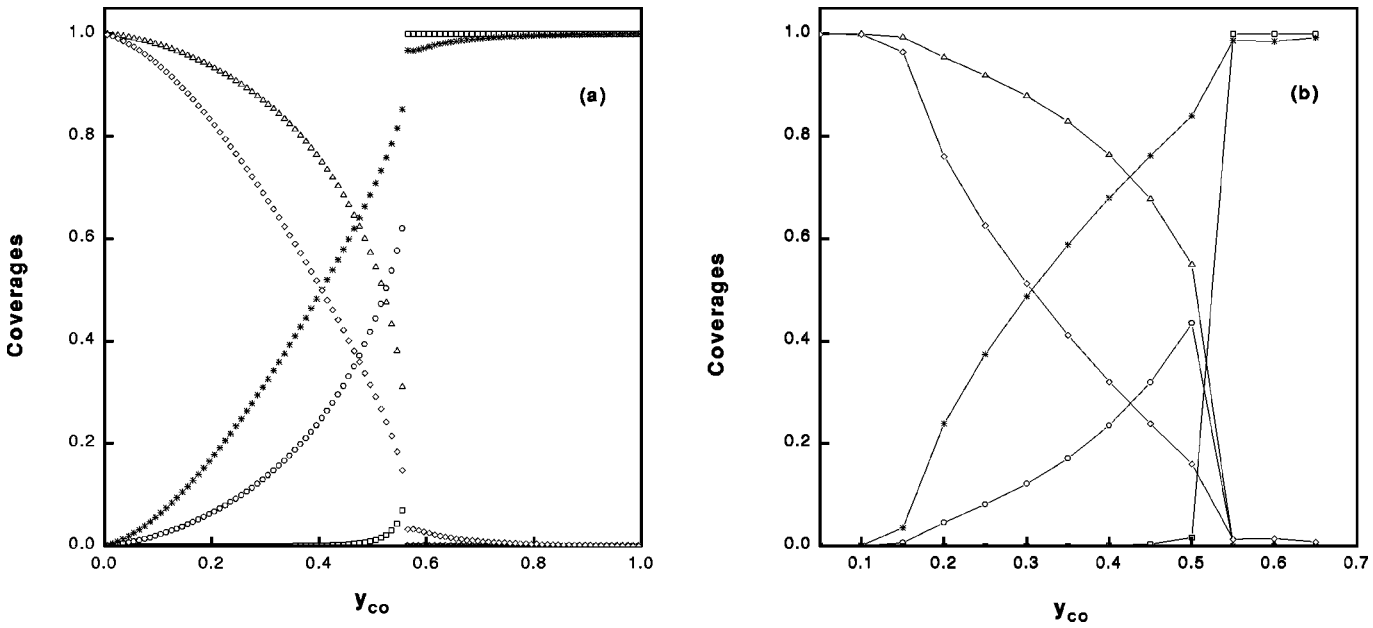


FIG. 2. The same legend as in Fig. 1. (a) Pair approximation with $d_1=0.1$ and $d_2=0.3$, and (b) Monte Carlo simulations with $d_1=0.1$ and $d_2=0.5$ (the curves serve as guides to the eye).

the number of trials of deposition of CO and $O_2$ molecules over the top layer ($L^2$ trials) plus $d_1L^2$ trials of diffusion of O from the top layer to the subsurface plus $d_2L^2$ trials of diffusion of O from the subsurface to the uppermost layer. For each sample, after the system reaches the stationary states, $10^4$ MCu were used to evaluate the coverages of interest.

Figure 1(b) exhibits the results of the simulations for the coverages, using the same values of $d_1$ and $d_2$ as in Fig. 1(a). The same features observed in the pair approximation calculation of Fig. 1(a) are found here. The critical value for the continuous transition between the reactive state and the O-poisoned state is $y_1=0.37$, which is very near to the one found by Ziff, Gulari, and Barshad in the absence of diffusion. This happens because in Fig. 1(b) the diffusion parameters are very small. On the other hand, when the upward diffusion coefficient $d_2$ increases, the continuous transition disappears above a given critical value. For instance, Fig. 2(a) shows the pair approximation coverages for a value of $d_2$ above its critical value: for any finite value of $y_{CO}$, the surface always contains a nonzero fraction of vacant sites. The continuous transition observed in Fig. 1(a) is no longer present for these values of the diffusion coefficients. As the upward diffusion coefficient $d_2$ is large, the coverage of oxygen atoms at the subsurface decreases faster than that one at the surface. Despite the large value of $d_2$, the first-order transition point does not change. The same behavior is also found within Monte Carlo simulations, as we can see in Fig. 2(b), although the diffusion parameters are different from those of Fig. 2(a).

In Figs. 3(a) and 3(b), we display the phase diagram in the plane $d_1$ versus $d_2$, where the continuous transition line separates regions with O-poisoned from non-O-poisoned states. In the pair approximation, Fig. 3(a), for values of $d_2$ larger than $d_{2c}=0.23$, it is not possible to find the surface poisoned by oxygen, whatever the value of $d_1\neq 0$. In the Fig. 3(b), we also plot the results obtained from Monte Carlo simulations. The behavior is the same observed in the pair approximation calculations, although the value we found for $d_{2c}$ is somewhat different. We have found that for $d_2>1.9$, the surface cannot be poisoned by oxygen atoms for any value of $d_1>0$.

Finally, Figs. 4(a) and 4(b) show the window width as we change the diffusion rates $d_1$ and $d_2$. In Fig. 4(a), we take a fixed value for $d_1$ and we change the upward diffusion rate $d_2$. Both, pair approximation calculations and Monte Carlo simulations, show an opening of the window width as we increase the value of $d_2$. The maximum window width is reached for the value of $d_{2c}$ as determined in Fig. 3. The value of $y_2$ is insensitive to the values of the diffusion rates in both calculations, although the Monte Carlo results predict a lower value than the one found within the pair approximation. In Fig. 4(b), we exhibit the plots of the window width obtained in both calculations for a fixed value of $d_2$, as a function of the downward diffusion rate $d_1$. As we can see, the widths decrease from a maximum value, which corresponds to the region where the surface is not poisoned by O [see Figs. 3(a) and 3(b) for the critical values], to a fixed value that no more depends upon $d_1$.

## IV. CONCLUSIONS

In summary, we have shown that with a slight modification of the ZGB model, which includes subsurface diffusion of oxygen atoms, it is possible to account for the experimental result concerning the absence of O-poisoned states in the oxidation of CO. These results were obtained by using the pair mean-field approximation and Monte Carlo simulations. In our approach we did not need to consider reaction steps involving the oxygen atom in the subsurface, which appears

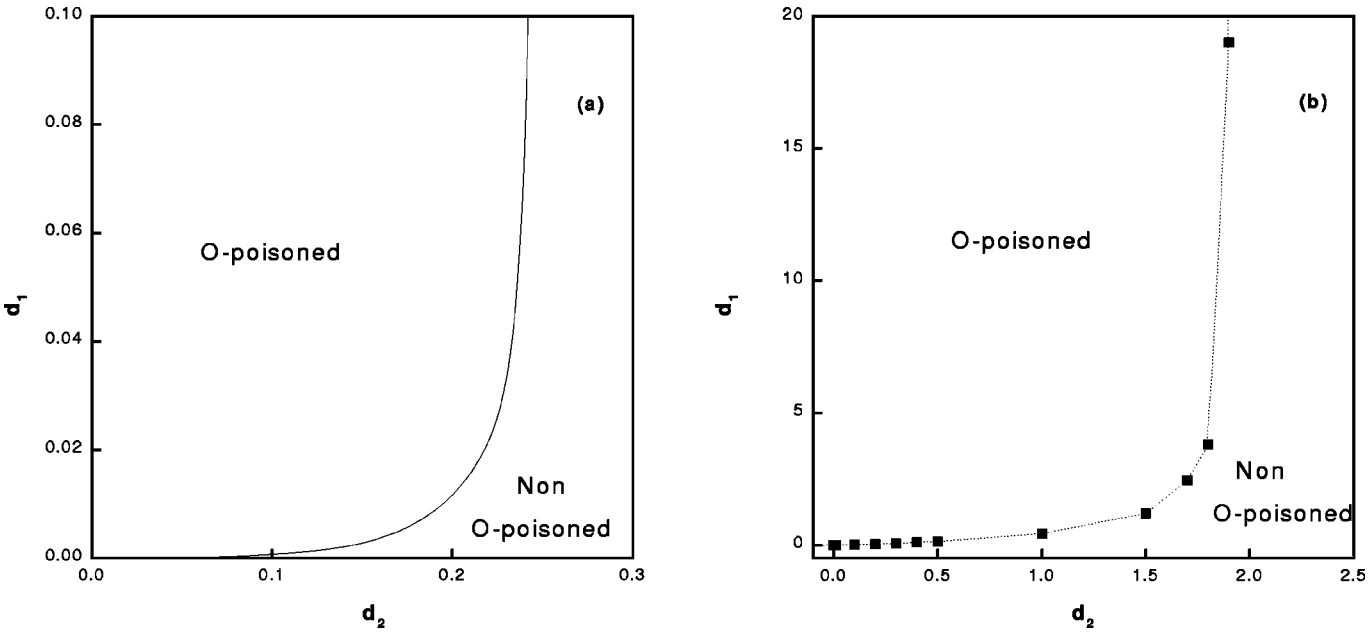


FIG. 3. Phase diagram in the plane $d_1$ (downward diffusion coefficient) versus $d_2$ (upward diffusion coefficient). (a) Pair approximation and (b) Monte Carlo simulations (the curve serves as a guide to the eye).

to be nonphysical. We have obtained a transition line that separates regions exhibiting O-poisoned states from non-O-poisoned states. Besides, we have seen that above a critical value of the upward diffusion coefficient, whose value depends on the approach we use, the surface cannot be found in an O-poisoned state.

## ACKNOWLEDGMENTS

This work was supported by the Brazilian agencies CNPq and FINEP.

## APPENDIX: TRANSITION RATES IN THE PAIR APPROXIMATION

Here we present the transition rates, derived in the pair approximation, amongst the possible pairs of nearest neighbors in the lattice, as indicated in Table I. For details of the procedure employed, see the appendixes of Dickman *et al.* [13]. In the following expressions, a site that is not occupied by a given element $\epsilon$ is represented by $\not{\epsilon}$. For instance, we write $p_{\not{C}V}$ to indicate a pair probability where one site is vacant ($V$) and the other cannot be occupied by CO. In this

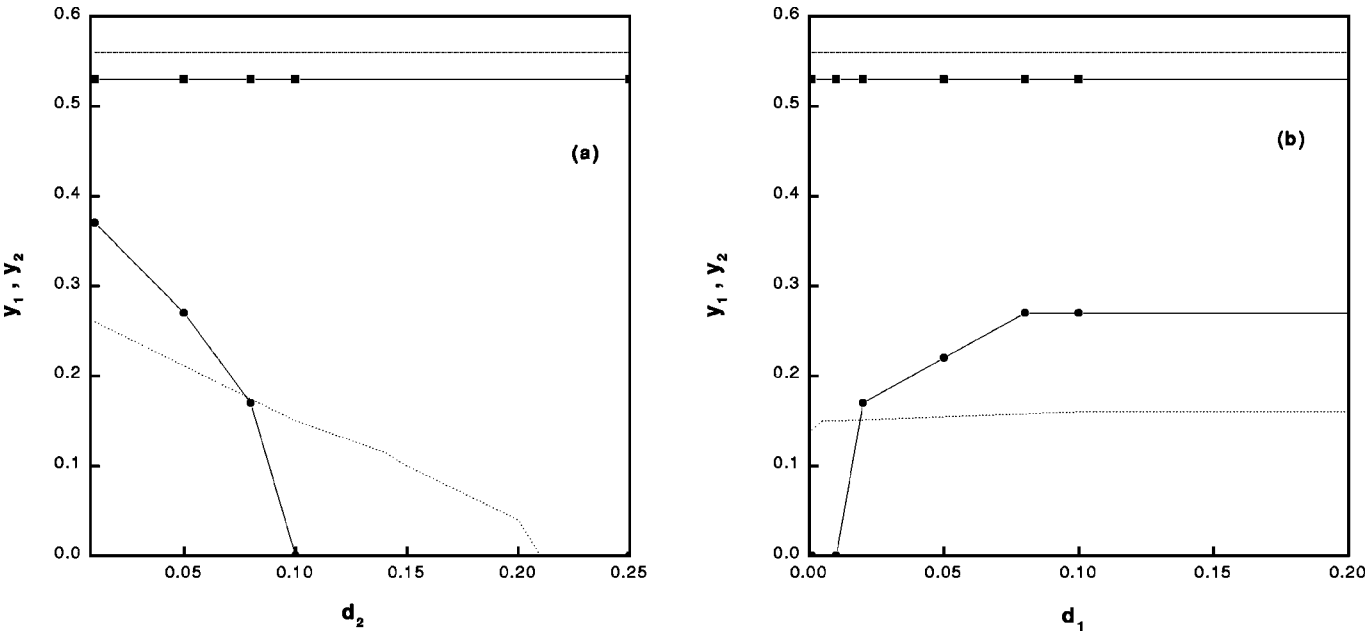


FIG. 4. (a) Transition points, $y_1$ (continuous) and $y_2$ (first order), as a function of $d_2$ for the fixed value of $d_1=0.01$. (b) Transition points, $y_1$ (continuous) and $y_2$ (first order), as a function of $d_1$ for the fixed value of $d_2=0.1$. $y_1$, dotted line (pair approximation) and circles (Monte Carlo simulations); $y_2$, dashed-dotted line (pair approximation) and squares (Monte Carlo simulations).

way, we have

$$p_{\varnothing V}=p_V-p_{VO},$$

$$p_{\complement V}=p_V-p_{VC},$$

$$p_{\complement C}=p_C-p_{CC},$$

$$p_{\varnothing O}=p_O-p_{OO}.$$

If we also define

$$\alpha=\tfrac{1}{4}p_{VO}^3+p_{\varnothing V}p_{VO}^2+\tfrac{3}{2}p_{\varnothing V}^2p_{VO}+p_{\varnothing V}^3,$$

we can write the following expressions for the transition rates:

$$R_1=(3p_{VC}/p_C+1)/p_V^3 3(1-y_{CO})p_{VC}p_{VV}(\tfrac{1}{3}p_{VC}^2+p_{\complement V}p_{VC}+p_{\complement V}^2)+(3p_{VC}/p_C+1)/p_V^4$$
$$\times d_2 p_{VC}p_{VO_S}(\tfrac{1}{4}p_{VC}^3+p_{\complement V}p_{VC}^2+\tfrac{3}{2}p_{\complement V}^2p_{VC}+p_{\complement V}^3),$$

$$R_2=y_{CO}p_{VO}\alpha(3p_{VO}/p_O+1)/p_V^3+d_1p_{VO}p_{OV_S}/p_O,$$

$$R_3=2(1-y_{CO})p_{CC}p_{VC}^2(\tfrac{1}{3}p_{VC}^2+p_{\complement V}p_{VC}+p_{\complement V}^2)^2/(p_V^4p_C^2),$$

$$R_4=y_{CO}p_{VV}p_{\varnothing V}^3/p_V^3,$$

$$R_5=(1-y_{CO})p_{CC}p_{VC}(\tfrac{1}{3}p_{VC}^2+p_{\complement V}p_{VC}+p_{\complement V}^2)[2(\tfrac{2}{3}p_{VC}^2+p_{\complement V}p_{VC})p_{VC}/(p_Vp_C)+3p_{VV}]/(p_V^3p_C)+[\tfrac{1}{3}p_{VC}p_{CC}+\tfrac{1}{2}(p_{\complement V}p_{CC}$$
$$+p_{VC}p_{\complement C})+p_{\complement V}p_{\complement C}]4(1-y_{CO})p_{CC}p_{VC}p_{VV}/(p_V^2p_C^2)+[\tfrac{1}{4}p_{VC}^2p_{CC}+\tfrac{1}{3}(2p_{VC}p_{\complement V}p_{CC}+p_{\complement C}p_{VC}^2)]$$
$$\times 2d_2p_{CC}p_{VC}p_{VO_S}/(p_V^3p_C^2)+[\tfrac{1}{2}(2p_{\complement V}p_{\complement C}p_{VC}+p_{\complement V}^2p_{CC})+p_{\complement V}^2p_{\complement C}]2d_2p_{CC}p_{VC}p_{VO_S}/(p_V^3p_C^2)+d_2p_{CC}p_{VC}p_{VO_S}(\tfrac{1}{4}p_{VC}^3$$
$$+p_{\complement V}p_{VC}^2+\tfrac{3}{2}p_{\complement V}^2p_{VC}+p_{\complement V}^3)/(p_V^4p_C),$$

$$R_6=(1-y_{CO})p_{VV}p_{\complement V}^2[p_{\complement V}(1-p_{\complement V}^3/p_V^3)+3p_{VV}]/p_V^3+d_2p_{VV}p_{VO_S}p_{\complement V}^3/p_V^4,$$

$$R_7=[\tfrac{1}{4}p_{VO}^2p_{OO}+\tfrac{1}{3}(2p_{VO}p_{\varnothing V}p_{OO}+p_{VO}^2p_{\varnothing O})]2y_{CO}p_{OO}p_{VO}/(p_V^2p_O^2)+[\tfrac{1}{2}(2p_{VO}p_{\varnothing V}p_{\varnothing O}+p_{\varnothing V}^2p_{OO})$$
$$+p_{\varnothing V}^2p_{\varnothing O}]2y_{CO}p_{OO}p_{VO}/(p_V^2p_O^2)+y_{CO}p_{OO}p_{VO}(\tfrac{1}{4}p_{VO}^3+p_{VO}^2p_{\varnothing V}+\tfrac{3}{2}p_{VO}p_{\varnothing V}^2+p_{\varnothing V}^3)/(p_V^3p_O)+d_1p_{OO}p_{OV_S}/p_O,$$

$$R_8=4y_{CO}p_{OO_S}p_{VO}\alpha/(p_V^3p_O),$$

$$R_9=d_1p_{OV_S},$$

$$R_{10}=9(1-y_{CO})p_{O_SC}p_{VC}p_{VV}(\tfrac{1}{3}p_{VC}^2+p_{VC}p_{\complement V}+p_{\complement V}^2)/(p_V^3p_C),$$

$$R_{11}=12(1-y_{CO})p_{CV_S}p_{VC}p_{VV}(\tfrac{1}{3}p_{VC}^2+p_{VC}p_{\complement V}+p_{\complement V}^2)/(p_V^3p_C)+4d_2p_{CV_S}p_{VC}p_{VO_S}(\tfrac{1}{4}p_{VC}^3+p_{VC}^2p_{\complement V}$$
$$+\tfrac{3}{2}p_{VC}p_{\complement V}^2+p_{\complement V}^3)/(p_V^4p_C),$$

$$R_{12}=4y_{CO}p_{OV_S}p_{VO}\alpha/(p_V^3p_O),$$

$$R_{13}=y_{CO}p_{VC}p_{\varnothing V}^3/p_V^3,$$

$$R_{14}=y_{CO}p_{VV_S}p_{\varnothing V}^4/p_V^4,$$

$$R_{15}=(1-y_{CO})p_{VV}p_{\complement V}^6/p_V^6,$$

$$R_{16}=3(1-y_{CO})p_{VO}p_{VV}p_{\complement V}^2/p_V^3+d_2p_{VO}p_{VO_S}p_{\complement V}^3/p_V^4,$$

$$R_{17}=4(1-y_{CO})p_{VO_S}p_{VV}p_{\complement V}^3/p_V^4,$$

$$R_{18}=d_2p_{VO_S},$$

$$R_{19}=4(1-y_{CO})p_{VV_S}p_{VV}p_{\complement V}^3/p_V^4,$$

$$R_{20}=d_1 p_{V_S V_S} p_{OV_S}/p_{V_S},$$

$$R_{21}=d_2 p_{O_S O_S} p_{VO_S}/p_{O_S},$$

$$R_{22}=d_2 p_{O_S V_S} p_{VO_S}/p_{O_S},$$

$$R_{23}=y_{CO} p_{VO_S} p_{\emptyset V}^4/p_V^4,$$

$$R_{24}=d_1 p_{O_S V_S} p_{OV_S}/p_{V_S}.$$


[1] R.M. Ziff, E. Gulari, and Y. Barshad, Phys. Rev. Lett. **56**, 2553 (1986).

[2] F. Bagnoli, B. Sente, M. Dumont, and R. Dagonnier, J. Chem. Phys. **94**, 777 (1991).

[3] P. Meakin and D.J. Scalapino, J. Chem. Phys. **87**, 731 (1987).

[4] I. Jensen and H.C. Fogedby, Phys. Rev. A **42**, 1969 (1990).

[5] E.V. Albano, Phys. Rev. Lett. **69**, 656 (1992).

[6] J. Satulovsky and E.V. Albano, J. Chem. Phys. **97**, 9490 (1992).

[7] K.M. Khan, K. Yaldram, J. Khalifeh, and M.A. Khan, J. Chem. Phys. **106**, 8890 (1997).

[8] J. Cortes, E. Valencia, and P. Araya, J. Chem. Phys. **109**, 5607 (1998).

[9] V.S. Leite, B.C.S. Grandi, and W. Figueiredo, J. Phys. A **34**, 1967 (2001).

[10] P.C. D'Ajello, P.R. Hauser, and W. Figueiredo, Physica A **293**, 83 (2001).

[11] R. Dickman, Phys. Rev. A **34**, 4246 (1986).

[12] H. Zhonghuai, Y. Lingfa, and X. Houwen, Phys. Rev. E **58**, 234 (1998).

[13] A.G. Dickman, B.C.S. Grandi, W. Figueiredo, and R. Dickman, Phys. Rev. E **59**, 6361 (1999).